JPE 6-2-4

Simulation and Experimentals of a Bi-Directional Converter with Input PFC on SRM System

Maged N. F. Nashed†

†Electronics Research Institute, Cairo, Egypt

ABSTRACT

This paper presents the performance and efficiency of a drive system incorporating a switched-reluctance motor (SRM) with input power factor correction (PFC). The proposed system consists of a PFC, bi-directional converter, an inverter, and a SRM operating as based voltage source drives (VSD). First, theoretical analysis is made for each identified mode of operation in the drive system. This is followed by comparing the performance of the SRM drive system with and without a PFC circuit. The losses are also calculated for both systems and overall efficiency. Experimental results are presented to prove the theoretical analysis.

Keywords: Bi-directionalal converter, Charger/Discharger with Batteries, C-dump converter, Power factor correction and inverter with SRM-based VSD

1. Introduction

Increasing the use of VSDs in industries and homes has brought to the forefront the important issue of reliability. Reliability is a function of drive topology, motor, converter components, control strategy and the availability of input power. The UPS connects the VSD system to alternate sources of energy such as batteries, fuel cells, internal combustion engine generator systems, solar arrays and/or a combination of them, when the utility power becomes unavailable. UPSs[1] are expensive and complex as they are designed to substitute the utility power source at a constant frequency. Constant frequency is ideal for constant speed drives, but not necessarily the optimal choice for VSD applications. VSD systems inherently require variable voltage/current and variable frequency in the case of induction and synchronous motor drives. In the case of chopper controlled DCM and SRM drives, the requirement is only a dc source, as opposed to an ac source. It becomes apparent that the inverter stage in a UPS is not required for VSD applications. This fact is of enormous consequence as it becomes obvious that for Bi-directional converters[2], it is not necessary to connect the UPS to the input power source, but to integrate it into the drive system.

The proposed system is of interest in many applications such as textiles, paper, critical applications in semiconductors, medical applications, freezer/ refrigerator drives, essential defense applications, garage doors, and sump pump motor drives. In home applications, VSDs are likely to enter the market due to high efficiency and energy-saving aspects. In this paper, the proposed system consists of four different functional modules: an input

Manuscript received August 8, 2005; revised February 22, 2006
†Corresponding Author: maged@eri.sci.eg
Tel:+202-33510552, Fax: +202-3370931, ERI

module which includes a diode bridge rectifier, a charger and discharger module implemented by a conventional buck/boost scheme, a battery module and an inverter based SRM drive module. The ratings of the converter are based on the analysis for a given SRM capacity. The system is analyzed for different operating modes and proved in experiments. The experimental efficiency studies, along with the VA ratings of the bi-directional converter are compared to conventional VSD systems. The system can be divided into two modes of operation: one at charging and the other when discharging batteries (see Fig. 1). Fig. 2 shows the buck converter while charging. The boost converter while discharging is shown in Fig. 3.

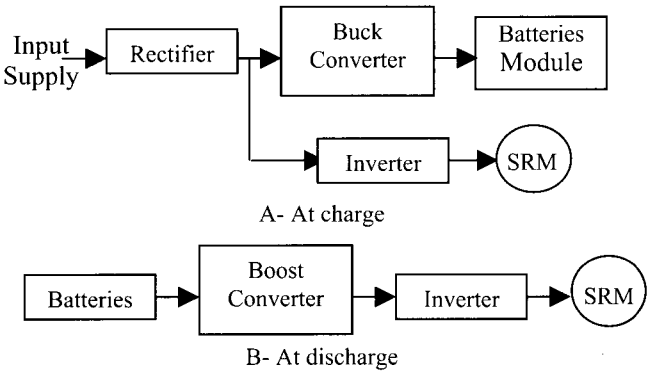

Fig. 1 The system at charge and discharge

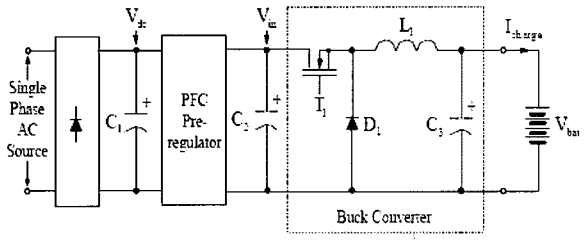

Fig. 2 Buck Converter as a charger

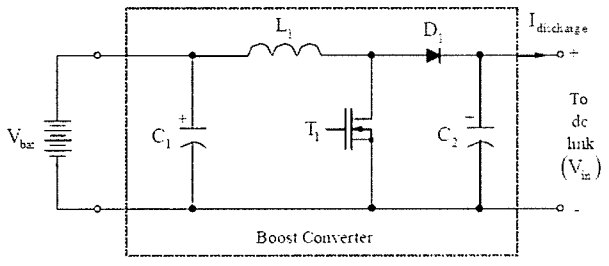

Fig. 3 Boost Converter as a discharger

2. Comparison of Switch VA Ratings of The Bi-Directional Converter

The dc link voltage and rated dc link current, considered base values for voltage and current, respectively, are used in comparing the charging and discharging modes. Considering only the VA rating of the power device, a comparison of the charger and discharger topologies is given in Table 1. The voltage ratio between the dc link and battery is a factor of n. It is assumed the battery charging switch rating current is 10% of its rated value. D denotes the duty cycle of the switch. A PFC with a buck configuration has a larger switch VA rating requirement, and thus may not be worth consideration for cost sensitive applications[3,4].

Table 1 Charger and discharger switch VA rating

Topology	V_{T1} pu	I_{T1} pu	P_{sw} pu
Charger	1.1	$0.1n\sqrt{d}$	$0.22n\sqrt{d}$
Charger with PEC	1.1	$0.1n\sqrt{d}$	$0.11n\sqrt{d}$
Discharger	1.1	$n\sqrt{d}$	$1.1n\sqrt{d}$

3. SRM-Based VSD as a Bi-Directional Converter System

The basic SRM-based VSD system as a bi-directional converter is illustrated in Fig. 4. The proposed bi-directional converter consists of four different functional modules: an input module which includes a diode bridge rectifier and PFC preregulator, a charger and discharger module implemented by a conventional buck/boost scheme, a battery module and a C-dump converter based SRM drive module[5]. Note that the charger unit, which is implemented with the buck topology, comes in both versions - with and without the PFC preregulator. The buck and boost converter is chosen based on its utility power readiness. A smooth transition is made possible due to the energy stored in the dc link capacitor. It would be able to supply the drive system until the boost comes on fully to meet the load requirement. Charging of the battery is controlled by the current

limiting loop, so it does not exceed the upper preset level. The voltage loop regulates the voltage at the preset level. The charger unit is approximately 10% of the battery VA capability due to low current charging which is preferred for longer battery life.

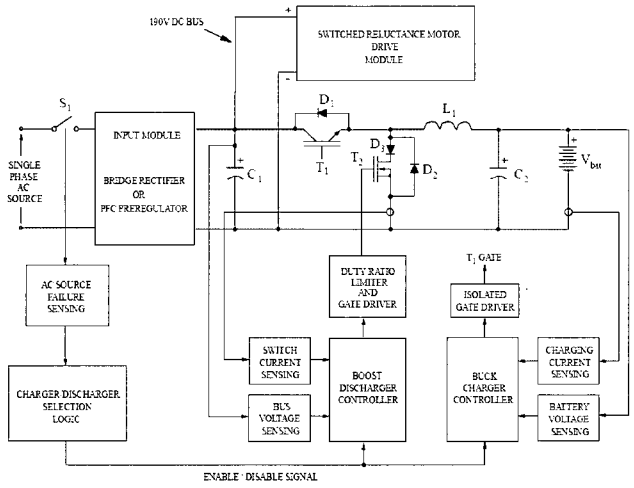

Fig. 4 The simplified block diagram of the proposed Bi-directional converter

The discharger unit has a boost power converter with an inner current limit circuit to protect the power switching device. It also contains a voltage loop to maintain the dc link voltage of the SRM drive system at the desired level. The duty ratio limit circuit is employed to set the maximum boost gain to five when there is a 20% drop in battery voltage. A C-dump converter, shown in Figure 5. The C-dump converter gives the most flexible control of the motor with the least number of switching devices [6, 7].

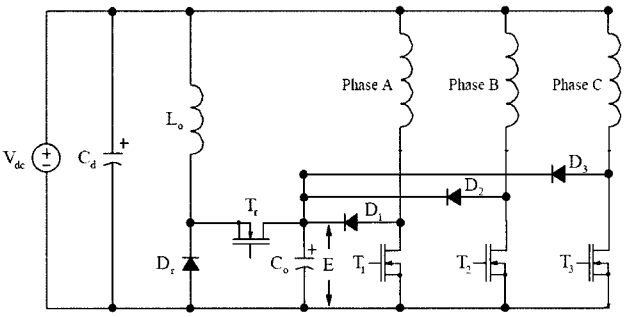

Fig. 5 Single switch per phase converter with C-dump energy recovery circuit

4. Analysis of Charger/Discharger Circuit

A bi-directional charger/discharger circuit is implemented with a combination of buck and boost converters for charger and discharger, respectively. The basic circuit is illustrated in Fig. 6. ote that the power inductor L_1 is shared between both converters, thus saving space. The motor drive is represented as the equivalent resistive load, R_{LOAD}, which is a function of the motor speed. T_1 is the buck switch implemented with an IGBT switching device, and D_2 is the freewheeling diode for the buck charger. The MOSFET boost switch, T_2, is operating with the boost diode D_1. The battery module is modeled as a resistor in series with a voltage source. There are two distinct operational states in both charging and discharging modes. The relationship between these states is defined in Fig. 7. The charger/discharger scheme implemented in this study operates in the discontinuous conduction mode because its average inductor current, I_{chg} in charging mode or I_{dcg} in discharging mode, is less than half of the inductor ripple current, Δi_L. T_s is the switching period in charging or discharging mode. d_1 corresponds to switch on time and d_2 relates to the freewheeling time of a diode in both charger and discharger circuits.

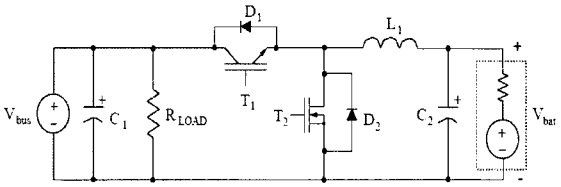

Fig. 6 Simplified circuit diagram of the proposed charger/discharger

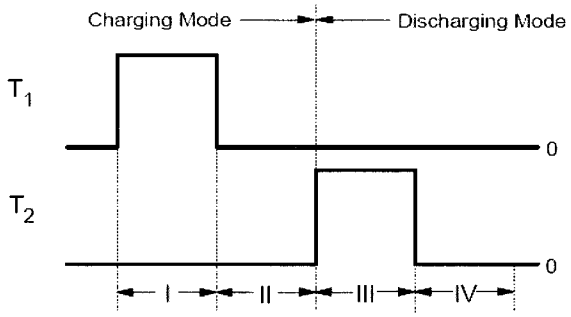

Fig. 7 Four operational modes of the proposed charger/discharger

The operational modes of the charger/discharger circuit are explained and expressions of the duty cycles and peak current are derived as follows:

4.1 Mode 1 : T_1 on and T_2 off

This mode occurs in the battery charging mode. Both the motor drive power and the battery charging power are supplied by the bus voltage, V_{bus} which is considered an input source. There are two current paths in this mode. The expressions for the battery charging current, $i_{ch}(on)$, and the bus current, i_{bus}, in this operational mode are as follows:

$$i_{ch(on)} = \frac{(V_{bus} - V_{bat})}{L_1} d_{1buck} T_{sbuck} \quad (1)$$

$$i_{bus} = i_L + i_{ch(on)} \quad (2)$$

Where, i_L is the load current supplied to the SRM drive.

4.2 Mode 2 : Both T_1 and T_2 off

When the buck switch T_1 is turned off, then the charging power is supplied by the energy stored in L_1. The power for the motor drive load is supplied by the bus voltage. The buck mode charging operation continues until the source power is interrupted. There are two current paths: one is the battery charging current, which is freewheeling through diode D_2 and inductor L_1, and the other one is the bus current supplying the SRM drive. The bus current is equal to the load current in this mode.

$$i_{ch(off)} = \frac{V_{bat}}{L_1} d_{1buck} T_{sbuck} \quad (3)$$

$$i_{bus} = i_L \quad (4)$$

The peak inductor current in charging mode is evaluated as,

$$i_{pkbuck} = \frac{d_{2buck} V_{bat}}{f_{cbuck} L_1} \quad (5)$$

The ratings and losses for key power components in the buck charger are summarized in Table 2.

4.3 Mode 3 : T_2 on and T_1 off

When the source power is turned off, the converter immediately enters the discharging mode. The first mode in the discharging operation is Mode III. The power for the motor drive is supplied by the energy stored in the bus capacitor only. The battery voltage is shorted through the boost inductor by the boost switch, T_2, to store the energy into the boost inductor. Two distinct currents in this mode are,

Table 2 ratings and losses for key power components

Device	Duty cycle	Ratings			Losses	
		Voltage	Peak Current	RMS Current	Conduction	Switching
Buck switch	d_{1buck}	V_{bus}	I_{pkbuck}	$I_{pkbuck}\sqrt{\frac{d_{1buck}}{3}}$	$I_{sw(rms)}V_{CE(Sat)}$	$0.5V_{in}$ I_{pkbuck} $f_{cbuck}(t_{rIGBT}+t_{fIGBT})$
Freewheeling Diode	d_{2buck}			$I_{pkbuck}\sqrt{\frac{d_{2buck}}{3}}$	$I_{drms}V_f$	$E_{rr}f_{cbuck}$
Inductor at buck	1			$I_{pkbuck}\sqrt{\frac{d_{1buck}+d_{2buck}}{3}}$	$I^2_{Lrms}R_{dc}$	-
Boost switch	d_{1boost}		$I_{pkboost}$	$I_{pkboost}\sqrt{\frac{d_{1boost}}{3}}$	$\frac{1}{2}I^2_{swrms}R_{dson}+I_{swrms}V_f$	$0.5V_{bus}I_{pkboost}$ $f_{cboost}(t_{rM}+t_{fM})$
Freewheeling diode	d_{2boost}			$I_{pkboost}\sqrt{\frac{d_{2boost}}{3}}$	$I_{drms}V_f$	$E_{rr}f_{cbuck}$
Inductor at buck	1			$I_{pkboost}\sqrt{\frac{d_{1boost}+d_{2boost}}{3}}$	$I^2_{Lrms}R_{dc}$	-

$$i_{dis(on)} = \frac{V_{bat}}{L_1} d_{1boost} T_{sboost} \quad (6)$$

$$i_L = C_1 \frac{V_{bus}}{d_{1boost} T_{sboost}} \quad (7)$$

4.4 Mode 4 : Both T_2 and T_1 off

The power for the motor drive is supplied by the battery only. The low battery voltage is boosted up to the original bus voltage level. Boost switch, T_2, and diode, D_1, provide the boost action along with the inductor, L_1. Note that the direction of the current is reversed.

$$i_{dis(off)} = \frac{(V_{bat} - V_{bus})}{L_1} d_{1boost} T_{sboost} \quad (8)$$

The peak current of the boost inductor is expressed as:

$$i_{pkboost} = \frac{d_{1boost} V_{bat}}{f_{cboost} L_1} \quad (9)$$

With the above equations, the ratings and losses of the major power components in the boost discharger are tabulated in Table 2.

Where,

$V_{CE(sat)}$ = collector-to-emitter saturation voltage of an IGBT switch , Volt

t_{riGBT} = rise time of an IGBT switch, sec.

t_{fiGBT} = fall time of an IGBT switch, sec.

V_f = forward voltage drop of freewheeling diode, Volt

E_{rr} = reverse recovery energy of freewheeling diode, J

R_{dc} = dc resistance of inductor, Ω

$R_{ds(on)}$ = static drain-to-source on-resistance of a MOSFET switch, Ω

t_{rM} = rise time of a MOSFET switch, s

t_{fM} = fall time of a MOSFET switch, s

5. Switched Reluctance Motor

In a switched reluctance motor, both stator and rotor have different magnetic reluctance along various radial axes. The SRM has six poles on the stator and four on the rotor. SRM electromechanical model can be represented by the following equations:

$$V = RI + d\psi/dt$$

And the angle between phases is

$$\theta_s = 2\pi (1/N_r - 1/N_s)$$

$$T_e = \frac{d}{d\theta} \int_0^i \psi \, di$$

$$J \, d\omega/dt = T_e - T_L$$

Where,

V is the terminal phase voltage,

I is the phase current,

R is the phase winding resistance,

ψ is the rotor flux linkage of phase,

N_r and N_s are the number of rotor and stator poles, respectively

T_e is the electrical torque = $1/2 \, i^2 \, dL/dt$

T_L is the load torque

J is the moment of inertia

And ω is the actual speed.

A simplified block diagram of the C-dump converter -based SRM drive is shown in Fig. 8. The proposed SRM drive system consists of a C-dump converter, which is shown, in Fig. 5, and a three phase SRM with an 8-bit absolute encoder. The control circuit of the C-dump consists of the main and auxiliary PWM controllers, This section is concerned with the design procedures of PI speed and current control circuits for the VSD system.

A simplified block diagram of the generalized VSD system with speed and current loops is illustrated in Fig. 9[5].

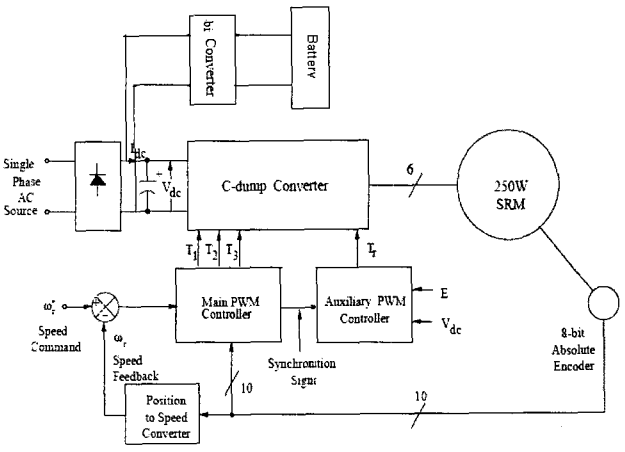

Fig. 8 Block diagram of the proposed Bi-directional converter and C-dump based SRM drive system

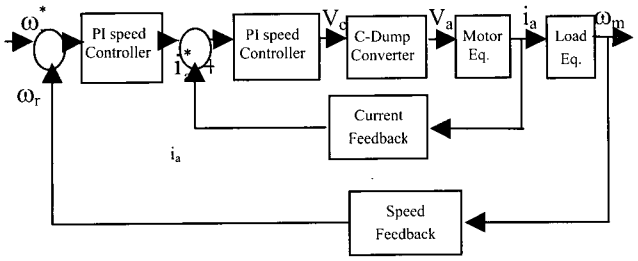

Fig. 9 Generalized block diagram of a closed-loop VSD system with current and speed feedback

The operation of a VSD system with speed and current control loops is as follows: the speed command, ω_r^*, is compared with the sensed speed feedback signal, ω_r, and applied to the speed PI controller. The output of the PI speed controller is the current command, i_a^*. The current error signal, which is the difference between the command and the sensed current, becomes the control voltage, V_c through PI current controller circuit. V_c is converted to a PWM switching signal and applied to the converter. The output of the converter block is the motor voltage, V_a, which is applied to the motor winding. The inner current loop governs the performance of the closed loop VSD system because its bandwidth is wider than the one in the outer speed loop. The wide bandwidth of the current loop ensures the stable operation and fast dynamic response of the VSD system. The current feedback gain has a constant value unless a low pass filter, which represents similar transfer function as a filter in speed feedback loop, is used.

6. System Simulation

The Matlab-Simulink package was used to simulate the proposed system. Simulation of the motor was based on equations 10 and 13 and on the tables of torque as functions of angle and current, and current as a function of angle and flux linkage. Due to partial derivatives equation solutions, these tables were constructed from the numerical data of a motor design finite elements program [8] to avoid time consumption. This three-dimensional data is illustrated in Fig. 10 and Fig. 11. All system simulations are performed in Matlab-Simulink. Fig. 12 shows the gate drive signals for charging and discharging.

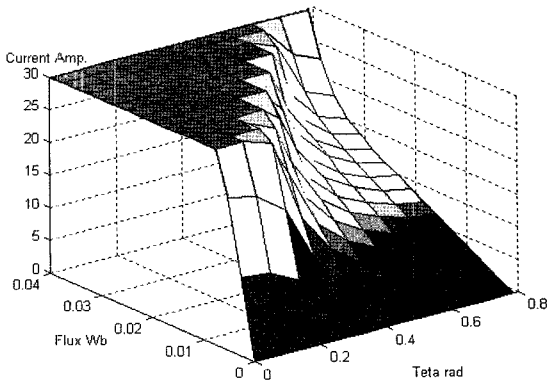

Fig. 10 phase Current data versus flux and rotor position for SRM

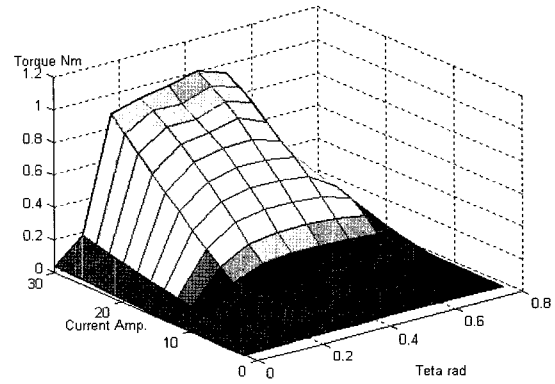

Fig. 11 Torque data versus motor phase current and rotor position for SRM

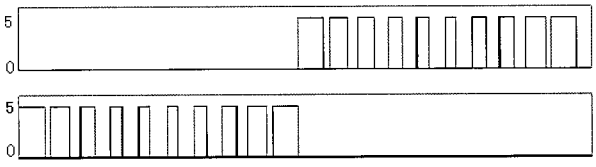

Fig. 12 Gate drive signals for charger and discharger

Fig 13 shows the phase voltage of the SRM when the duty cycle of the boost converter is increased and then the speed and torque is also increased at a constant current (under current control). Fig. 14 shows the phase current and voltage and rotor position. While Fig. 15 shows the phase current and torque with the change of the reference control of the current. Fig. 16 shows the phase torque for three phases of the motor.

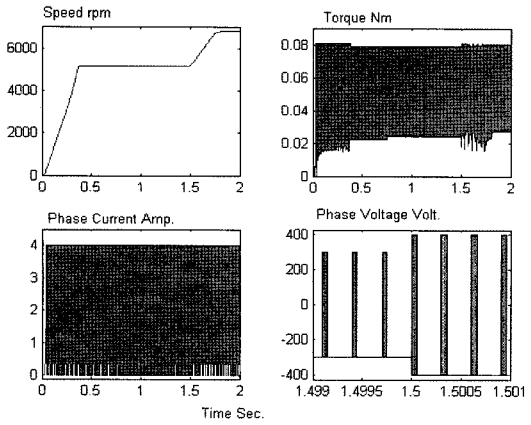

Fig. 13 phase voltage, speed, torque and phase current of the SRM when the duty cycle of boost converter is increased

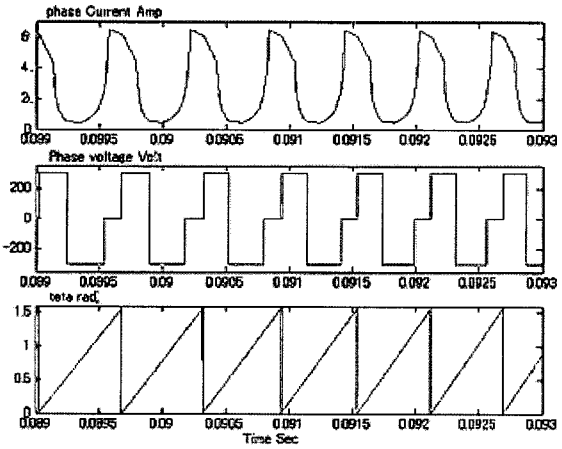

Fig. 14 Phase current and voltage and rotor position of the SRM

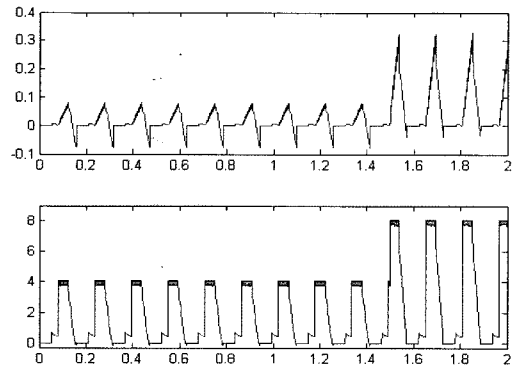

Fig. 15 Phase current and torque with the change of the reference control of current

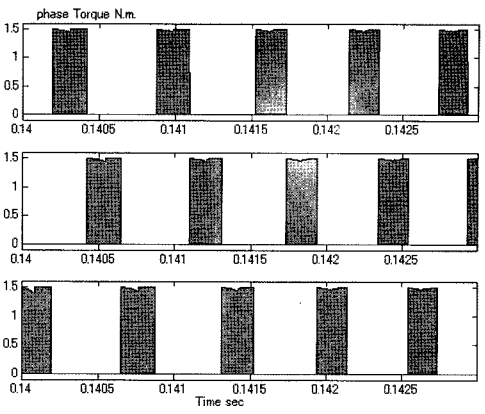

Fig. 16 the three phase torque of SRM

7. Experimental Verification

A simplified block diagram of the experimental system is shown in Fig.17. The C-dump converter for the SRM drive is MOSFET-based. The charger is built using an IGBT switch and tested with and without a PFC. The battery module consists of four series connected, sealed, lead-acid rechargeable batteries; each having a 12V and 7Ah rating. A permanent-magnet brush dc generator with a resistive bank serves as the load for the SRMdrive system. The losses of the dc generator, as a function of speed and current, have been experimentally predetermined. Therefore the input to the dc generator is equal to the output of the SRM-based VSD, which consists of power dissipated in the resistive bank and losses in the dc generator.

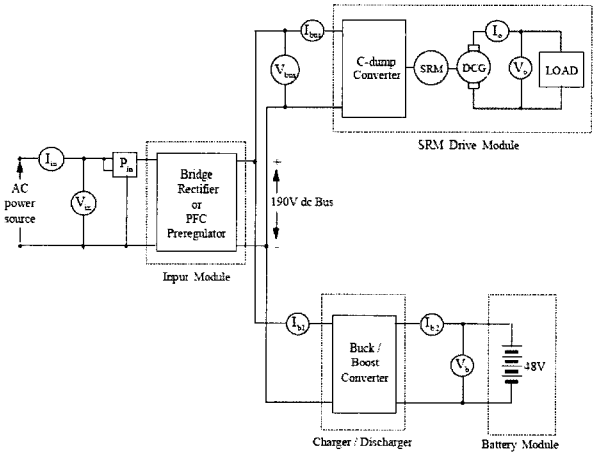

Fig. 17 Experimental test setup for bi-directional converter system with SRM-based VSD

The various measurements for obtaining efficiencies in charging and discharging modes are taken from 100r/min to 2,000r/min with 100r/min speed increments. The experimental results are focused on the functioning of the bi-directional converter system, proper operation of the charger and discharger modules. Fig.18 shows the gate drive signals of the buck/boost switches before and after power failure with no power to the converter (see the simulation in Fig.12). V_{g1} is the gate signal, isolated by the pulse transformer for charger switch T_1[9], and V_{g2}, directly connected to the gate of the boost switch T2. The current in one phase of the motor is shown in Fig. 19. Charging/discharging currents as seen through the inductor in the buck/boost charger/discharger converter modules in the charging mode and the discharging mode are also shown. Note that the charging and discharging actions are taken in two different instances. The charging current has a peak of 2A. This is because the dc link voltage is near 190V, whereas the battery module is at 48V nominal input. The discharging current reaches a peak of 7A, but due to the short discharge duration, the peak is nearly 3.5 times the current required for the drive system. Fig. 20 shows the three phases of the motor torque.

During charging mode, the utility input power supplies the power for the SRM drive and charges power for the battery module as shown in Fig. 1(a). The overall efficiency is the ratio between the sum of the charging power and the SRM's output to input power[10]. The system efficiency, evaluated for the bi-directional converter with and without PFC, is shown in Fig. 21(a) and (b) as a function of motor speed. Both efficiencies closely match over the entire power output range. The efficiency of the system without the PFC circuit has been consistently high, by a margin of 5%, throughout the entire speed range when compared to the case with the PFC. This is because the PFC contains losses in its control circuit with active and passive devices over and above that of the diode bridge rectifier. Hence its losses are higher than the simple diode bridge rectifier circuit, contributing to poorer overall system efficiency throughout the speed region. To increase the efficiency of the overall system during this time, it is important to have the discharger module operating at high efficiency.

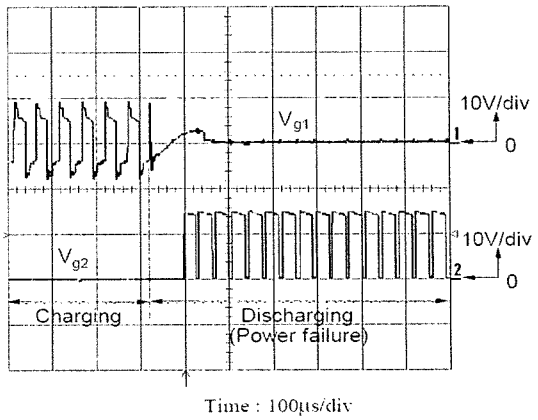

Fig. 18 Transient gate drive signals for charger/discharger

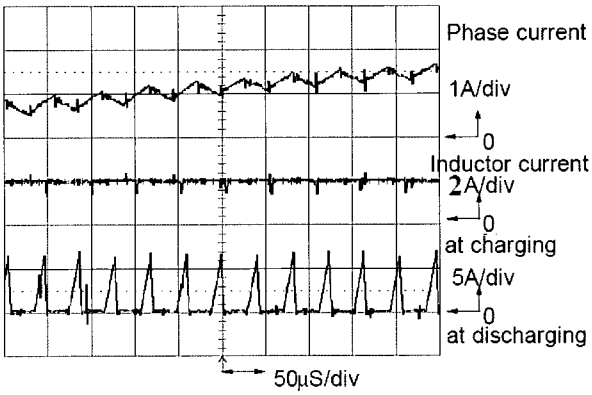

Fig. 19 Current waveforms of SRM phase and inductor in charger/discharger at 1,000r/min

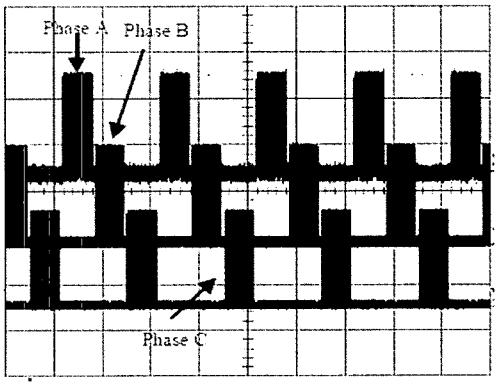

Fig. 20 Experimental for three phase torque of SRM

The overall system efficiency during the discharging mode is defined as the ratio between the SRM's output and the battery module's output. As shown in Fig. 22, the efficiency is lower than the charging mode by nearly 7%.

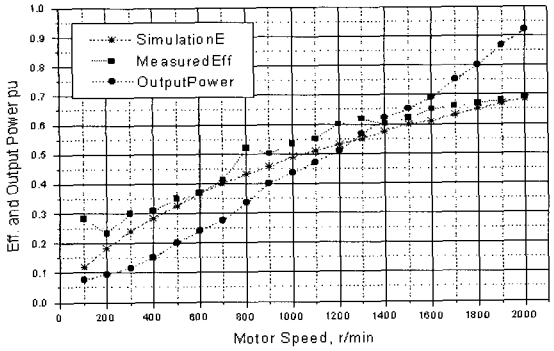

(a) Without PFC

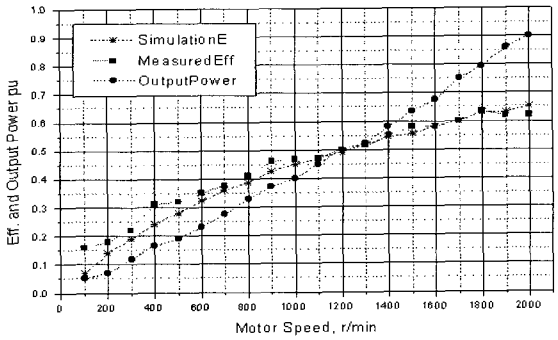

(b) With PFC

Fig. 21 Overall system efficiency and normalized output power in charging mode

This is caused by factors such as higher losses in the boost converter due to the higher pulse currents involved during this mode. The power supply for the PFC is always connected to the bus, lowering the overall system efficiency slightly. Efficiency with the PFC is lower than that of the simple diode bridge case because the control logic keeps drawing power from the dc link even during its off mode.

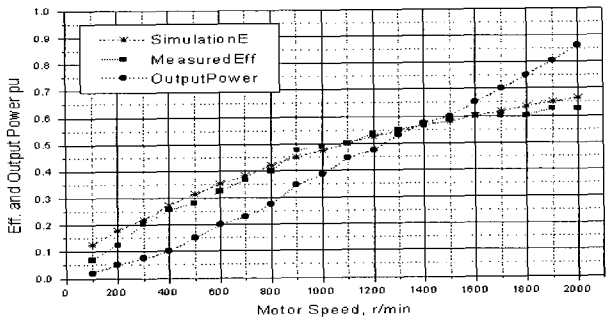

Fig. 22 Overall system efficiency and normalized output power in discharging mode without PFC

8. Conclusions

Inclusion of the input PFC to SRM-based VSD systems has been proposed for appliance applications. Its performance has been verified in experiments, analysis and simulations. Operational modes of the proposed VSD systems have been identified and analytical derivations are made for each mode. Based on this, the system equations and design procedures are systematically derived to evaluate the drive system performances with and without an input PFC pre-regulator. A comparison of drive performance with input PFC shows its overall system efficiency is consistently lower than that without an input PFC. This decrease in efficiency has to be weighted against the advantages of the near sinusoidal current from utility, high power factor and reduction of input current harmonics of the input PF-corrected drive system. Integration of an input PFC is recommended with a clear understanding that it will lower the overall system efficiency. The bi-directional converter concept was proposed and illustrated with a C-dump converter based SRM drive system. Various topologies for bi-directional converters were analyzed and experimentally verified. Overall system performance and efficiency of input PFC to SRM-based VSD systems were experimentally and analytically evaluated and found to be acceptable for many applications.

References

[1] R. Krishnan and S. Srinivasan, "Topologies for Uninterruptible Power Supplies," IEEE International Symposium on Industrial Electronics, Budapest, Hungary, June 1-3, 1993.

[2] R. Krishnan and S. Lee, " Uninterruptible Motor Drives: A Case Study With Switched Reluctance Motor Drives," IEEE IECON Conf. Italia, Sept.1994.

[3] J. Lee, G. Moon, and M. Youn "Design of a Power Factor Correction Converter based on Half Bridge Topology" IEEE Transactions on Industrial Electronics Vol. 46, No. 4, Aug. 1999.

[4 C. Klumpner, P. Nielsen, I. Boldea, and F. Blaabjerg "By new solutions for a low-cost power electronic building block for matrix converters" IEEE Transactions on Industrial Electronics, Vol. 49, No. 2, April 2002.

[5] T. Miller, "Switched Reluctance Motors and their Control", Magna Physics Publishing and Clarendon Press-Oxford, 1993.

[6] M. Ehsani, J. Bass, T. Miller, and R. Steigerwald, "Development of a unipolar converter for variable reluctance motor drives", IEEE Transactions on Industry Applications, Vol.IA-23, No.3, May/June 1987.

[7] S. Vukosavic, and V. Stefanovic, "SRM inverter topologies: A comparative evaluation", IEEE Transactions on Industry Applications, Vol.27, No.6, Nov/Dec. 1991.

[8] K. Ohyama, M. N. F. Nashed, K. Aso, H. Fujii, and H. Uehara "Design Using Finite Element Analysis of Switched Reluctance Motor for Electric Vehicle" Asian Electric Vehicle Conf.-4, Nov. 26-28, Osaka, Japan, 2005.

[9] N. Mohan, T. Undeland and W. Robbins, "Power Electronics: Converters, Applications, and Design," John Wiley & Sons, Inc., 1989.

[10] P. Materu, and R. Krishnan, "Estimation of switched reluctance motor losses", IEEE Transactions on Industry Applications, Vol. 28, No. 3, May/June 1992.

Maged Naguib Fahmy Nashed received B. S. degrees in Electrical Engineering, from the univ. of Menoufia University, Egypt, in May 1983, the Diploma of Higher from Cairo University, May 1990, the M. SC. Degree in Electrical Engineering, from Ain shams University, Cairo, Egypt, in April 1995 and the Ph. D. of degree in Electrical Engineering, from Ain -shams University, Cairo, Egypt, in January 2001. He research for 6 months in Fukuoka Institute of Technology, Japan, 2005. Since 1989, he has been with the Dept. of Power Electronic and Energy conversion. Electronic Research Institute, where he is currently a Researcher. He is engaged in research on Power Electronic, Drive circuit, control of drives and Renewable Energy.